

Fluctuation-Phase Relation between Positive and Negative Ions on Pair-Plasma Electrostatic Waves

W. Oohara, D. Date, and R. Hatakeyama

Department of Electronic Engineering, Tohoku University Sendai 980-8579, Japan

Abstract. Three kinds of electrostatic modes are experimentally observed to propagate along magnetic-field lines for the first time in the pair-ion plasma consisting of only positive and negative fullerene ions with an equal mass. It is found that phase lags between the density fluctuations of positive and negative ions vary from 0 to π depending on the frequency and is fixed at π in the cases of ion acoustic and ion plasma waves, respectively. In addition, a new mode with the phase lag about π appears in an intermediate-frequency band between the acoustic and plasma waves.

PACS numbers: 52.27.Ep, 52.35.Fp, 81.05.Tp

1. Introduction

Plasmas comprising assemblies of charged particles, which interact with each other through the Coulomb force, are known to reveal various kinds of unique properties. A typical plasma consists of electrons and positive ions, and the mass difference between negative- and positive-charged particles essentially causes temporal and spatial varieties of collective plasma phenomena. As one of the phenomena, linear and nonlinear properties of electrostatic and electromagnetic waves have been investigated in plasmas so far. Pair plasmas consisting of only positive- and negative-charged particles with an equal mass have been investigated experimentally [1–7] and theoretically [8–14], since the pair plasmas, such as electron-positron plasma, are thought to be generated naturally under certain astrophysical conditions. Both the relativistic and non-relativistic pair-plasmas are gradually disclosed to represent a new state of matter with unique thermodynamic property drastically different from ordinary electron-ion plasmas. A comprehensive analysis of the elementary properties of the pair plasmas, linear- and nonlinear-collective plasma modes, has theoretically been developed and the experimental identification is at present desired to be performed. However, the identification of the collective modes is very difficult in the electron-positron plasmas because the annihilation time is short compared with the plasma period. Therefore our attention is concentrated on the stable generation of a pair-ion plasma consisting of positive and negative ions with an equal mass and the resultant collective-mode identification.

According to our previous work on the generation of an alkali-fullerene plasma (K^+ , e^- , C_{60}^-) by introducing fullerenes into a potassium plasma [15–18], fullerenes are adopted as a candidate for the ion source in order to realize the pair-ion plasma, based on the fact that the interaction of electrons with the fullerenes leads to the production of both negative [19, 20] and positive [21–23] ions. We have developed a novel method for generating the pair-ion plasma which consists of only positive and negative ions with an equal mass using fullerenes [24], and discussed basic characteristics of the pair-ion plasma in terms of the differences from ordinary electron-ion plasmas. Here the pair-ion plasma source is drastically improved in order to increase the plasma density and excite effectively the collective modes. We mainly present properties of the electrostatic modes propagating along magnetic-field lines.

2. Pair-Ion Plasma Generation

The improved pair-ion source with ion species of fullerenes is installed in a grounded vacuum-chamber of 15.7 cm in diameter and 260 cm in length, as shown schematically in Fig. 1 [24]. A uniform magnetic field of $B = 0.3$ T is applied by solenoid coils and the background gas pressure is 2×10^{-4} Pa. A grounded copper cylinder (8 cm in diameter and 30 cm in length) with a copper annulus (3 cm in inner diameter, 8 cm in outer diameter, and 0.1 cm in thickness) is fixed inside a cylindrical ceramic furnace and

heated to 500 °C. An electron-beam gun is set inside the copper cylinder, which consists of four tungsten wires connected electrically in parallel. This wire cathode heated over 2000 °C by resistive heating is biased at a voltage V_k (< 0 V) with respect to a grounded grid set at less than 0.5 cm in front of the cathode. A stainless-steel disk of 4 cm in diameter is concentrically welded onto the gridded anode. Thermionically emitted low-energy electrons (~ 0.2 eV) are accelerated by an electric field between the cathode and anode, forming a hollow electron beam. The beam flows along magnetic (B) field lines and is terminated at the grounded annulus. The beam energy E_e can be controlled in the range of 0–150 eV by changing V_k . The cylinder and the ceramic furnace have a hole (3 cm in diameter) on the sidewall and an oven for fullerene sublimation is set there, where a fullerene sample (C_{60} powder) is heated at a temperature between 400 and 600 °C. The fullerene vapor produced as a result of sublimation is effused through a 0.3-cm-diam hole under molecular flow conditions, filling the cylinder.

For analytic convenience, the whole space of this plasma is divided into three regions (I), (II), and (III), as shown in Fig. 1. The electron-beam region is called Region (I) as a fullerene-ion production region. Positive ions C_{60}^+ are produced by the electron-impact ionization and low-energy electrons are simultaneously produced in connection with this process. Negative ions C_{60}^- are produced by the attachment of these low-energy electrons. The attachment occurs over a very wide energy range, extending to about 12 eV, and which is deserving special mention. The gyroradius ratio between C_{60}^+ and electron $\rho_{C_{60}^+}/\rho_{e^-}$ is especially high ($\simeq 1100$), and a preferential ambipolar-diffusion of C_{60}^+ and C_{60}^- can take place in the radial (r) direction across the B -field lines, i.e., electrons are separated by a magnetic-filtering effect [25]. Only C_{60}^+ and C_{60}^- are expected to exist in the midmost of the cylinder, Region (II), and the electron-free pair-ion plasma generation is attained here. C_{60}^+ and C_{60}^- flow along the B -field lines and pass through the annular hole toward an experimental region, Region (III). The thick copper annulus (3 cm in inner diameter, 8 cm in outer diameter, and 3 cm in thickness) is set between Region (II) and (III), and independently biased at a dc voltage V_{an} and an ac voltage V_{exc} . The plasma density in Region (III) can be controlled by changing V_{an} and V_{exc} . The exit position of the thick annulus is defined as $z = 0$ cm, and the pair-ion plasma is terminated at a floating endplate ($z = 90$ cm). Plasma parameters in Region (III) are measured by Langmuir probes, collectors of which are prevented from being contaminated by C_{60} .

The generation property of the pair-ion plasma depending on the electron-beam energy E_e is measured at $r = 0$ cm and $z = 5$ cm in Region (III) for $V_{an} = V_{exc} = 0$ V, as shown in Fig. 2. I_+ and I_- are the Langmuir-probe saturation currents of C_{60}^+ and C_{60}^- , respectively, which are considered to be in proportion to the plasma density. When E_e increases from 0 eV, the pair-ion plasma begins to be generated. The plasma density once saturates, a little bit decreases around 9 eV, increases around 15 eV again, and finally attains to 1×10^8 cm $^{-3}$ at $E_e = 100$ eV. The temperatures of C_{60}^+ and C_{60}^- , T_+ and T_- , are about 0.5 eV. The plasma and floating potentials are almost 0 V which is equal to the potential of the grid and the thin annulus. Therefore it can be said that the static

potential-structures including sheaths are not formed in the pair-ion plasma because the ions have the same mass and temperature. This property of the plasma generation in the energy range of $E_e < 30$ eV is quite different from the previous result for the case of the LaB₆ cathode [24]. The plasma density in $E_e < 30$ eV does not clearly depend on the magnetic field B , but strongly depends in $E_e > 30$ eV. The direct contact of the fullerene vapor with the thermal cathode is supposed to be involved in the ionization process of fullerene, although the exact physical mechanism in $E_e < 30$ eV is not understood. Since the density in Region (III) drastically decreases for $|V_{an}| \neq 0$ V, the density modulation can be realized without using a grid immersed inside the plasma cross section, which disturbs the plasma condition. Thus, longitudinal-electrostatic modes are excited in the pair-ion plasma, when the voltage of the annular exciter is temporally alternated ($V_{exc} \neq 0$).

3. Electrostatic Waves in Pair-Ion Plasma

Some theoretical works have already been presented, which concern linear and nonlinear collective modes in non-relativistic electron-positron plasmas [8–13]. A comprehensive two-fluid model has been developed for collective-mode analyses, based on which longitudinal (transverse) electrostatic (electromagnetic) modes have been studied. The longitudinal collective modes are analogous to those in the ordinary electron-ion plasmas. On the other hand, the transverse collective modes in the presence of a magnetic field are quite different from those in the ordinary plasmas, for instance, the whistler mode does not exist. Here, electrostatic modes are focused in our pair-ion plasma, because the density and the temperature are relatively low and the induction current of the ions is very small, and electromagnetic modes relevant to the plasma can be neglected.

The twofluid equations in the absence of an applied B field appropriate to the pair-ion plasma consist of the usual momentum and continuity equations for each species, supplemented by Poisson's equation.

$$mn_j \left(\frac{\partial v_j}{\partial t} + (v_j \cdot \nabla) v_j \right) = -q_j n_j \nabla \phi - \gamma T_j \nabla n_j, \quad (1)$$

$$\frac{\partial n_j}{\partial t} + \nabla \cdot (n_j v_j) = 0, \quad (2)$$

$$\nabla^2 \phi = -\frac{e}{\varepsilon_0} (n_+ - n_-). \quad (3)$$

Where m , n_j , v_j , q_j , T_j , and ϕ denote the mass, the density, the fluid velocity, the charge, the temperature, and the potential, respectively. The subscript j denotes positive or negative ions, $j = +$ or $-$, γ is the ratio of specific heats, and ε_0 is the permittivity of free space. Linearizing about a homogeneous unbounded plasma (ion temperatures $T = T_+ = T_-$), and defining the phase lag between the density fluctuations of positive

and negative ions by $n_{+1} = n_{-1} \exp(i\theta)$ for clarity, the coupled linear mode-equations are derived:

$$\omega^2 - c_s^2 k^2 - (1 - \exp(-i\theta))\omega_p^2 = 0, \quad (4)$$

$$\omega^2 - c_s^2 k^2 - (1 - \exp(i\theta))\omega_p^2 = 0, \quad (5)$$

where the acoustic speed $c_s^2 = \gamma T/m$ and the plasma frequency $\omega_p^2 = e^2 n/\epsilon_0 m$ are introduced. The dispersion relations associated with Eqs. (4) and (5) are simply given by

$$\omega^2 = c_s^2 k^2 \quad (\theta = 0), \quad (6)$$

$$\omega^2 = c_s^2 k^2 + 2\omega_p^2 \quad (\theta = \pi). \quad (7)$$

These modes are the ion acoustic wave (6) and the ion plasma wave (7). In a nonzero applied B field but for which a zero magnetic fluctuation, the dispersion relations [13] are given by

$$(\omega^2 - \omega_p^2)(\omega^2 - c_s^2 k^2 - \omega_h^2) + c_s^2 \omega_c^2 k^2 \cos^2 \alpha = 0, \quad (8)$$

$$\omega^2(\omega^2 - c_s^2 k^2 - \omega_c^2) + c_s^2 \omega_c^2 k^2 \cos^2 \alpha = 0. \quad (9)$$

These modes propagating along B -field lines (α : propagation angle, $\alpha = 0$) is quite same as that in the absence of B field, except for the cyclotron oscillation ω_c and the upper hybrid oscillation $\omega_h = \sqrt{2\omega_p^2 + \omega_c^2}$.

The property of the wave propagation along the B -field lines is measured at $r = 0$ cm and $z = 10$ – 12 cm in Region (III) for $E_e = 100$ eV by exciting the density fluctuation with the annular exciter, as mentioned above. The measured (dots) and the calculated (solid curves) dispersion relations are shown in Fig. 3, where the density modulation condition is $V_{an} = 0$ V and $V_{exc} = 0.2$ V, and the resultant amplitude of the density fluctuation n_1/n_0 is about 0.1. The wave number (wave length) is obtained from the phase delay of the positive-ion density fluctuation measured at $z = 10, 11,$ and 12 cm. The theoretical curves are calculated using Eqs. (6) and (7) for $\gamma = 3$ (one-dimensional compression), $T = 0.5$ eV (isotropy), and $n_0 = 1 \times 10^7$ cm $^{-3}$. Typical plasma parameters are as follows: the pair-plasma frequency is $(\sqrt{2}\omega_p)/2\pi = 35$ kHz, the cyclotron frequency ($B = 0.3$ T) is $\omega_c/2\pi = 6.4$ kHz, and the acoustic speed is $c_s = 4.5 \times 10^4$ cm/s. There are three branches in the measured dispersion relation, $\omega/2\pi < 8$ kHz (the ion acoustic wave, IAW), $8 < \omega/2\pi < 32$ kHz, and $\omega/2\pi > 32$ kHz (the ion plasma wave, IPW). IPW measured fits to the calculated curve, and IAW measured in the relatively low-frequency band ($\omega/2\pi < 3$ kHz) also fits but deviates from it in the relatively high-frequency band ($3 < \omega/2\pi < 8$ kHz). It is worth while pointing out that a new mode is experimentally observed in $8 < \omega/2\pi < 32$ kHz for the first time, but we have not succeeded in deriving theoretically the dispersion relation of the new mode yet. The new mode has the feature that the group velocity is negative but the phase velocity is positive, i.e., the mode is like a backward wave, and called the intermediate-frequency wave (IFW) here.

The typical temporal variations of the positive- and negative-ion densities and the potential are presented for $\omega/2\pi = 0.4, 2$ kHz (IAW), 20 kHz (IFW), and 35 kHz (IPW) in Figs. 4 (a), (b), (c), and (d), respectively. \tilde{I}_+ , \tilde{I}_- , and $\tilde{\phi}_f$ indicate the oscillating components of the positive and negative saturation currents (relative to the positive- and negative-ion densities), and the floating potential of the probe (the space potential) measured at $z = 10$ cm, respectively. The frequency spectrum of the phase lag $\theta(\tilde{I}_-) - \theta(\tilde{I}_+)$ between \tilde{I}_+ and \tilde{I}_- is measured at $r = 0$ cm and $z = 10$ cm as shown in Fig. 5. In Fig. 4 (a), the phase lag of the densities for IAW is close to zero and the amplitude of the potential oscillation is extremely small, which is consistent with the result derived from the theoretical dispersion relation (6). Although the property of IAW measured in the very low-frequency range ($\omega/2\pi < 1$ kHz) is the same as the theoretical one, the phase lag starts to increase in proportion to $\omega/2\pi$ ($1 < \omega/2\pi < 3$ kHz) and attains to a constant value of about 1.1π ($3 < \omega/2\pi < 8$ kHz), which has not been explained theoretically yet. On the other hand the phase lags for IPW and IFW are π and 1.03π independently of $\omega/2\pi$, respectively, and their potential-oscillation amplitudes are large, as seen in Figs. 4 (c) and (d).

The modes propagating oblique B -field lines are observed in vicinity of the annular exciter. The measured (dots) and the calculated (solid curves) dispersion relations are shown in Fig. 6, where the mode is measured at $r = 0$ cm and $z = 2-4$ cm for $E_e = 100$ eV, $V_{an} = 0$ V, and $V_{exc} = 0.2$ V. Here, the wave number k_{\parallel} denotes the parallel component of k and the propagation angle is 0.48π with respect to B -field lines. The theoretical curves are calculated from Eqs. (8) and (9) for $\alpha = 0.48\pi$ and the plasma parameters are same as the case of propagating along B -field lines. There are four branches and the ion cyclotron resonance appears in the measured dispersion relation. A backward-wave like mode exists around the ion cyclotron frequency $\omega_c/2\pi$ ($= 6.4$ kHz) but not in the frequency range of between the ion acoustic wave and the ion plasma wave. The phase lag of the modes propagating oblique B -field lines will be measured in our future works.

Some theoretical ideas for providing an explanation of the modes are recently proposed, and we introduce them here. Dr. A. Hasegawa and Dr. P. K. Shukla suggest that the modes could be surface waves and they derive the dispersion relations of them in a planer model and a cylindrical model. Dr. H. Schamel suggests the interpretation of the wave characteristics in term of periodic hole equilibria and associated kinetic modes, where the mode coupling between the ion plasma wave and the ion acoustic wave is caused by the particles trapped in the wave potential and IFW could appear. Dr. F. Verheest suggests the oblique propagation of large amplitude electromagnetic solitons in pair plasmas. Dr. J. Vranjes suggests that only two modes, the electrostatic Langmuir mode and the electromagnetic transverse plasma mode, could exist in the pair-ion plasma in the absence of B field. We will make it appear experimentally that these theoretical suggestions are well suited to this pair-ion plasma or not.

4. Summary

In summary, for the purpose of experimentally investigating electrostatic wave phenomena in a pair-ion plasma, the drastic improvement of the pair-ion plasma source consisting of only C_{60}^+ and C_{60}^- with an equal mass is performed effectively using a magnetized hollow electron beam, and processes of electron-impact ionization, electron attachment, and magnetically-filtered separation. The active excitation of density modulation by a thick annulus reveals the existence of three kinds of electrostatic modes propagating along B -field lines, an ion acoustic wave (IAW), an ion plasma wave (IPW), and an intermediate-frequency wave (IFW). IAW and IPW are predicted in the twofluid theory for a unbounded plasma, while IFW is not predicted but only experimentally observed here. The phase lags between the density fluctuations of positive and negative ions are 0 for IAW in the low-frequency range, about π for IFW, and π for IPW.

Acknowledgement

The authors would like to thank T. Hirata and T. Kaneko for their collaboration. We are indebted to N. Tomioka, M. Kobayashi, and H. Iwata for their support. This work was supported by a Grant-in-Aid for Scientific Research from the Ministry of Education, Culture, Sports, Science, and Technology, Japan. Finally, we thank some theoreticians for their suggestions.

- [1] G. Gibson, W. C. Jordan, and E. J. Lauer, *Phys. Rev. Lett.* **5**, 141 (1960).
- [2] C. M. Surko, M. Leventhal, and A. Passner, *Phys. Rev. Lett.* **62**, 901 (1989).
- [3] C. M. Surko and T. J. Murphy, *Phys. Fluids B* **2**, 1372 (1990).
- [4] R. G. Greaves, M. D. Tinkle, and C. M. Surko, *Phys. Plasmas* **1**, 1439 (1994).
- [5] H. Boehmer, M. Adams, and N. Rynn, *Phys. Plasmas* **2**, 4369 (1995).
- [6] E. P. Liang, S. C. Wilks, and M. Tabak, *Phys. Rev. Lett.* **81**, 4887 (1998).
- [7] M. Amoretti et al, *Phys. Rev. Lett.* **91**, 055001 (2003).
- [8] G. A. Stewart and E. W. Laing, *J. Plasma Phys.* **47**, 295 (1992).
- [9] N. Iwamoto, *Phys. Rev. E* **47**, 604 (1993).
- [10] S. Y. Abdul-Rassak and E. W. Laing, *J. Plasma Phys.* **50**, 125 (1993).
- [11] G. A. Stewart, *J. Plasma Phys.* **50**, 521 (1993).
- [12] J. Zhao, K. I. Nishikawa, J. I. Sakai, and T. Neubert, *Phys. Plasmas* **1**, 103 (1994).
- [13] G. P. Zank and R. G. Greaves, *Phys. Rev. E* **51**, 6079 (1995).
- [14] D. H. E. Dubin, *Phys. Rev. Lett.* **92**, 195002 (2004).
- [15] J. P. Schermann and F. G. Major, *Appl. Phys.* **16**, 225 (1978).
- [16] N. Sato, T. Mieno, T. Hirata, Y. Yagi, R. Hatakeyama, and S. Iizuka, *Phys. Plasmas* **1**, 3480 (1994).
- [17] W. Oohara, R. Hatakeyama, and S. Ishiguro, *Plasma Phys. Control. Fusion* **44**, 1299 (2002).
- [18] W. Oohara, R. Hatakeyama, and S. Ishiguro, *Phys. Rev. E* **68**, 066407 (2003).
- [19] T. Jaffke, E. Illenberger, M. Lezius, S. Matejcik, D. Smith, and T. D. Märk, *Chem. Phys. Lett.* **226**, 213 (1994).
- [20] J. Huang, H. S. Carman, Jr., and R. N. Compton, *J. Phys. Chem.* **99**, 1719 (1995).
- [21] R. Völpel, G. Hofmann, M. Steidl, M. Stenke, M. Schlapp, R. Trassl, and E. Salzborn, *Phys. Rev. Lett.* **71**, 3439 (1993).

- [22] S. Matt, B. Dünser, M. Lezius, H. Deutsch, K. Becker, A. Stamatovic, P. Scheier, and T. D. Märk, *J. Chem. Phys.* **105**, 1880 (1996).
- [23] A. A. Vostrikov, D. Yu. Dubnov, and A. A. Agarkov, *High Temperature* **39**, 22 (2001).
- [24] W. Oohara and R. Hatakeyama, *Phys. Rev. Lett.* **91**, 205005 (2003).
- [25] D. P. Sheehan and N. Rynn, *Rev. Sci. Instrum.* **59**, 1369 (1988).

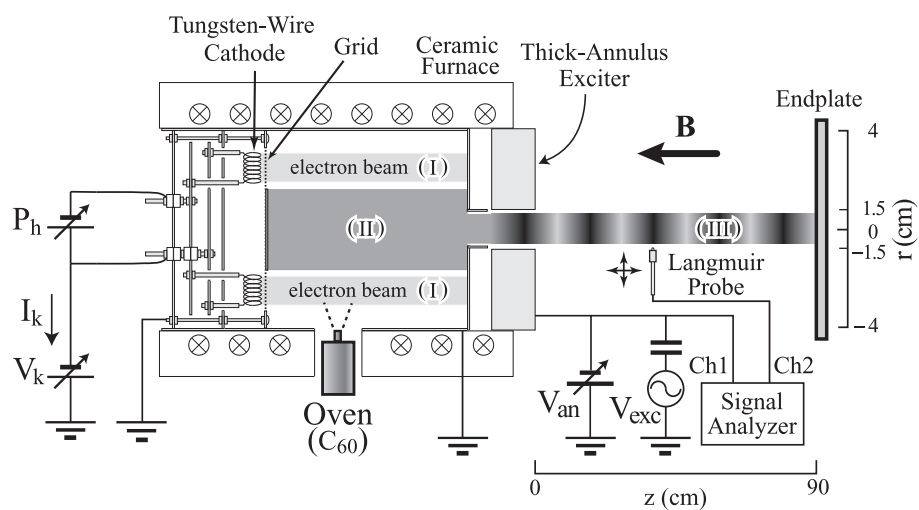


Figure 1. Schematic drawing of the experimental setup. Pure pair-ion plasma using fullerene (C_{60}^+ , C_{60}^-) is generated by electron-impact ionization, electron attachment, and magnetic filtering. Density modulation (longitudinal-electrostatic wave) is excited by thick annulus.

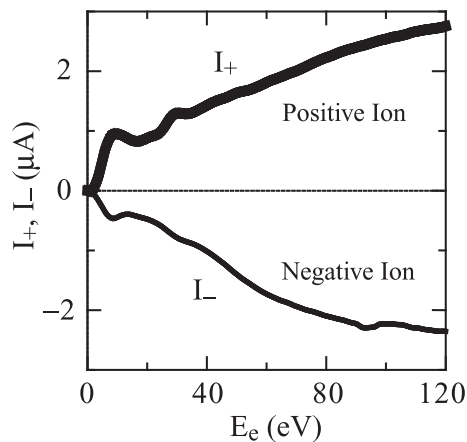


Figure 2. Generation property of pair-ion plasma depending on electron-beam energy E_e in Region (III).

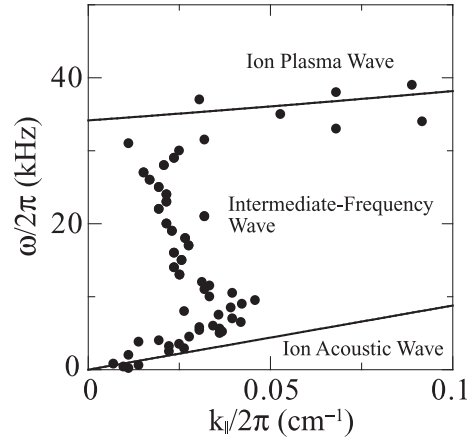


Figure 3. Dispersion relations for electrostatic waves propagating along B -field lines. Dots denote experimental results. Solid curves denote results calculated from Eqs. (6) and (7).

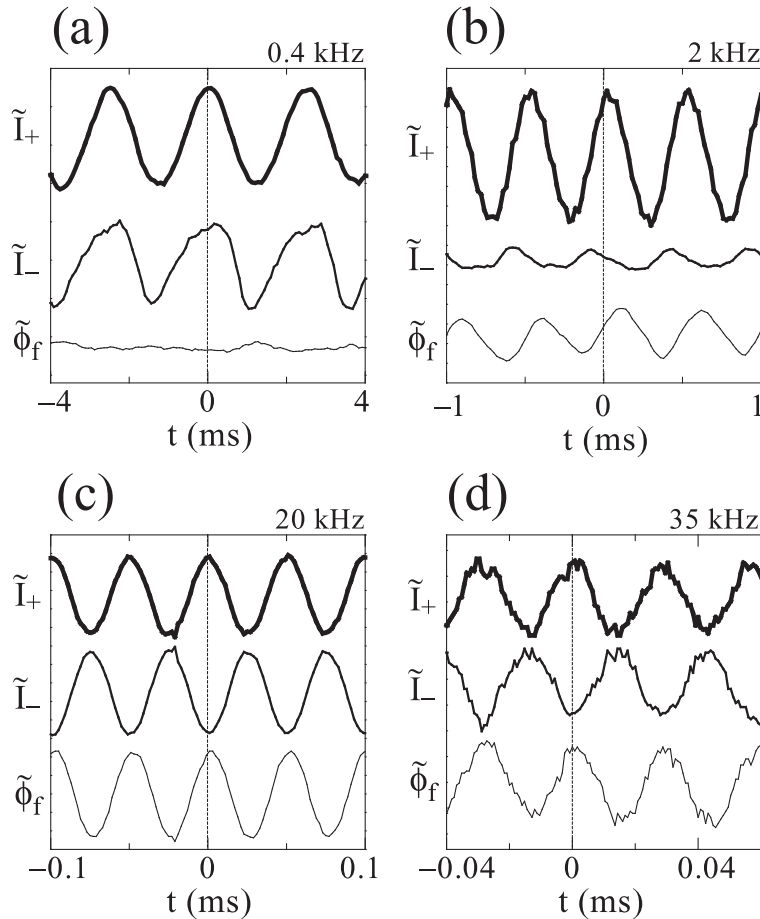


Figure 4. Typical temporal variations of positive- and negative-ion densities and potential at $\omega/2\pi =$ (a) 0.4 kHz, (b) 2 kHz, (c) 20 kHz, and (d) 35 kHz.

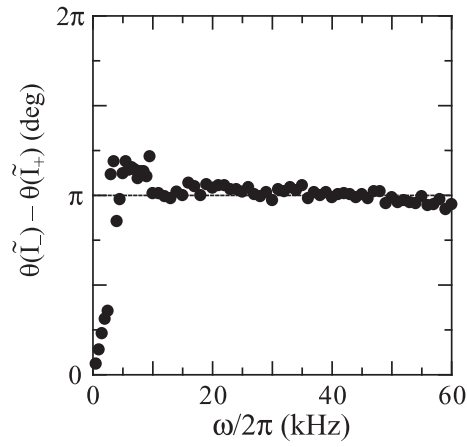


Figure 5. Frequency spectrum of phase difference between negative and positive density fluctuations propagating along B -field lines measured around $z = 10$ cm.

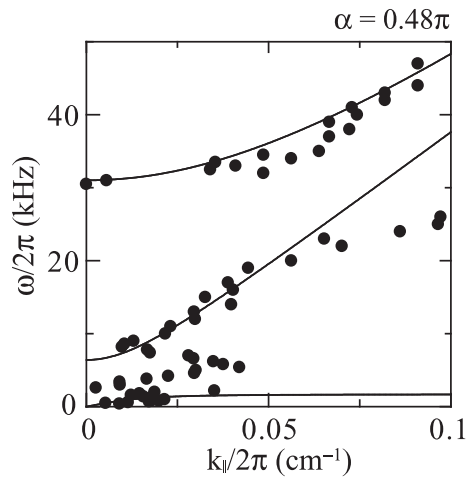


Figure 6. Dispersion relations for electrostatic waves propagating oblique B -field lines. Dots denote experimental results. Solid curves denote results calculated from Eqs. (8) and (9).